

Do Neural Networks Lose Plasticity in a Gradually Changing World?

Tianhui Liu¹ Lili Mou^{1,2}

Abstract

Continual learning has become a trending topic in machine learning. Recent studies have discovered an interesting phenomenon called loss of plasticity, referring to neural networks gradually losing the ability to learn new tasks. However, existing plasticity research largely relies on contrived settings with abrupt task transitions, which often do not reflect real-world environments. In this paper, we propose to investigate a gradually changing environment, and we simulate this by input/output interpolation and task sampling. We perform theoretical and empirical analysis, showing that the loss of plasticity is an artifact of abrupt tasks changes in the environment and can be largely mitigated if the world changes gradually.

1. Introduction

Continual learning has become a trending topic in machine learning research, where a system incrementally learns from non-stationary distributions (Ring, 1997; Ruvolo & Eaton, 2013; Shin et al., 2017; Kirkpatrick et al., 2017; Abbas et al., 2023). In supervised learning, a system is trained to perform isolated tasks (Thrun, 1998). However, training a system from scratch is onerous and time-consuming, especially for large neural networks (Dean et al., 2012). It would be more computationally and economically efficient to incrementally adapt them to new tasks.

Loss of plasticity is an intriguing phenomenon recently discovered in continual learning, referring to neural networks gradually losing the ability to learn new tasks (Dohare et al., 2021; 2024; Lyle et al., 2023; Zilly et al., 2021; Abbas et al., 2023; Lewandowski et al., 2025a). Proposed mitigation techniques include regularizing the model weights (Zilly et al., 2021; Lewandowski et al., 2024; 2025a; Kumar et al., 2023), using alternative activation functions (Berariu et al., 2021; Lee et al., 2023; Abbas et al., 2023), controlling the

¹Dept. Computing Science & Alberta Machine Intelligence Institute (Amii), University of Alberta ²Canada CIFAR AI Chair. Correspondence to: Tianhui Liu <tianhui17@gmail.com>, Lili Mou <doublepower.mou@gmail.com>.

loss landscape sharpness (Lyle et al., 2023), resetting less-used neurons (Dohare et al., 2024; Sokar et al., 2023), and selectively forgetting memorized noise (Shin et al., 2024).

However, we observe that these studies typically adopt a contrived setting, where the tasks change abruptly. For example, in image classification, tasks are often constructed by randomly assigning labels or permuting pixels (Dohare et al., 2024; Lyle et al., 2023; Lewandowski et al., 2024; 2025a). Then, the system is trained in different tasks one after another, which simulates a continually changing environment. Note that for each abrupt task transition, the system may not be aware of the task boundary.

It is therefore important to consider whether such contrived setting of abrupt task transitions reflects real-world continual learning. Consider the evolution of human language. Researchers show that the sense of a word may change from time to time, but this happens gradually, as the new and old senses typically co-exist during the change (Kilgarriff, 1997; Mitra et al., 2015; Laurino et al., 2023). For instance, the word “sick” traditionally refers to “illness” in standard English; however, it has recently adopted new meanings such as “cool” or “crazy” (Mitra et al., 2015). This shift marks a transition from a negative sense to a positive one, with both meanings currently being understood by the general public. Although findings on such a contrived setting are interesting by themselves, there is an imminent need to study the loss of plasticity in a more realistic setup where the task changes gradually. In this paper, we empirically and theoretically show that loss of plasticity is an artifact of abrupt changes in the environment (as hinted in (Abbas et al., 2023; Dohare et al., 2024; Lyle et al., 2024)) and can be largely mitigated if the world changes gradually. In our setting, we propose to perform input/output interpolation or task sampling to simulate a gradually changing environment. We observe that neural networks preserve plasticity magnitudes longer than those under abrupt task changes. Therefore, the problem of loss of plasticity ceases to be a major concern in general real-world applications of continual learning as the real-word data distributions shift gradually.

In certain scenarios where the tasks do change abruptly (e.g., robots in new environments), our work provides simple yet effective smoothing techniques, namely, interpolation and task sampling, to mitigate the loss of plasticity.

We provide an interpretation of why smooth task transitions mitigate plasticity loss. When tasks change abruptly, the error surface also changes abruptly; parameters learned for the previous task may then become trapped in a poor local optimum for the new task, making optimization difficult. However, a gradually changing environment induces smoother changes in the error surface, which can guide parameters toward a better optimum for the new task. We formalize this intuition through a theoretical analysis.

In addition, we conduct experiments on four tasks covering both trainability and generalizability (which are two aspects of plasticity). Our results indicate that a gradually changing environment preserves plasticity and matches the performance of existing mitigation methods.

Overall, our work brings new insights and opportunities to the research of loss of plasticity, particularly in formulating a realistic and practical setup.

2. Related Work

Plasticity represents a neural system’s adaptability to new environments. This mechanism has been a foundational subject in neuroscience for decades (Citri & Malenka, 2008; Rodriguez et al., 2009), but has only recently received growing attention in supervised classification and reinforcement learning (Dohare et al., 2021; 2024; Lyle et al., 2022; Sokar et al., 2023).

The loss of plasticity is an intriguing phenomenon observed in deep learning models, which can be categorized into two aspects: the neural network’s ability to train (Dohare et al., 2021; 2024; Lyle et al., 2022; Elsayed & Mahmood, 2024; Lewandowski et al., 2024; 2025b;a; Ma et al., 2024), and the ability to generalize (Dohare et al., 2024; Ash & Adams, 2020; Zilly et al., 2021; Lewandowski et al., 2025a; Lee et al., 2024; Anonymous, 2026). Early research primarily focuses on trainability, operating under the assumption that minimizing training loss is the principal objective. However, Ash & Adams find that neural networks initialized with pre-trained weights leads to faster convergence but worse generalization (Ash & Adams, 2020). This indicates that the network has become trapped in a low-generalization basin, memorizing without learning robust representations.

Prior studies have hypothesized different underlying causes of plasticity loss and proposed corresponding methods to preserve it. Loss of plasticity is initially attributed to dormant neurons (Sokar et al., 2023; Dohare et al., 2024), where the number of inactive neurons increases during training, effectively reducing network capacity. This problem can be directly mitigated by periodically resetting a subset of the neurons (Frati et al., 2024; Sokar et al., 2023). A second factor is optimizer instability (Lyle et al., 2023), as standard optimizers like Adam (Kingma & Ba, 2015) and

stochastic gradient descent (SGD) are designed for stationary data distributions. In continual learning, the optimizer state (e.g., momentum) becomes biased toward previous tasks; to address this, researchers have proposed periodic optimizer resets (Nikishin et al., 2022; Asadi et al., 2023) and layer normalization (Lyle et al., 2023) to alleviate plasticity loss. Prolonged training can also lead to a loss of curvature directions, characterized by rank collapse in the Hessian, which restricts directions available for future optimization (Lewandowski et al., 2024). Regularization methods are proposed to prevent model weights from deviating from the initial values, for instance, L2 regularization (Kumar et al., 2023; Lyle et al., 2022; Dohare et al., 2024), Wasserstein regularization (Lewandowski et al., 2024), and spectral regularization (Lewandowski et al., 2025a).

Additionally, loss of generalization in continual learning is often attributed to memorization. As training progresses, weight magnitudes increase, and the model tends to overfit—memorizing specific samples from previous tasks rather than learning generalizable features. The Shrink&Perturb method (Ash & Adams, 2020) mitigates this by scaling down weight magnitudes and injecting noise to reduce memorization. It aims to force the model selectively forget memorized noise while preserving learned features.

Moreover, recent work shows that carefully designed activation functions can effectively mitigate plasticity loss. Examples include Concatenated ReLUs (CReLU; Abbas et al., 2023), Smooth-Leaky activation families (Anonymous, 2026), and highly trainable deep Fourier features (Lewandowski et al., 2025b).

Several heuristic approaches have also been proposed, including smaller batch sizes (Obando Ceron et al., 2023), orthogonal parameter regularization (Chung et al., 2024), and reducing churn—unintended prediction drift induced by data outside the current batch (Tang et al., 2025).

It is important to notice that existing research on loss of plasticity assumes that the tasks change abruptly, which is less realistic in the real world. In our work, we investigate gradually changing environments, and show that loss of plasticity becomes less an issue. In addition, simulating a gradually changing environment by interpolation or task sampling can be a simple method that mitigates loss of plasticity (even if the tasks change abruptly).

3. Problem Formulation

The problem of loss of plasticity has recently been observed in continual learning when the data distribution in each sequentially coming task is changed rapidly and non-stationarily. In the continual learning literature, the concept of loss of plasticity can refer to either reduced ability to learn new from new data (loss of trainability) (Dohare et al.,

2021; Lyle et al., 2022; Elsayed & Mahmood, 2024; Ma et al., 2024), or reduced ability to generalize to unseen data (loss of generalizability) (Dohare et al., 2024; Ash & Adams, 2020; Lee et al., 2024; Zilly et al., 2021). Our work investigates the loss of plasticity problem from the perspective of both trainability and generalizability.

Let $\mathcal{D} = \{(\mathbf{x}_m, y_m)\}_{m=1}^M$ be a training dataset where $\mathbf{x}_m \in \mathbb{R}^d$ is an input sample (e.g., an image with d pixels) and $y_m \in \mathbb{Y}$ be the corresponding label. We denote a deep neural network by a function f_θ . The learning algorithm optimizes the parameters by minimizing the loss of each task, given by $\text{m, minimize}_\theta \mathbb{E}_{(\mathbf{x}, y) \sim p_t} [\ell(f_\theta(\mathbf{x}), y)]$. There are different settings in continual learning regarding the availability of samples in previous tasks. We adopt the common setting in the loss of plasticity research, where we assume the machine learning model is able to iterate over a task’s samples multiple times in a mini-batch fashion, although the task boundary is not informed (Li et al., 2014; Lewandowski et al., 2024; Lyle et al., 2022).

To further illustrate this process, we introduce two popular examples in the previous literature that simulate a continually changing environment.

Random Image Labeling. In this environment, the label of an image is randomly selected from $0, \dots, c$ where c is the number of classes in the dataset. In other words, the dataset of the t th task is $\mathcal{D}^{(t)} = \{(\mathbf{x}_m, y_m^{(t)})\}_{m=1}^M$, where \mathbf{x}_m comes from the original image dataset, and $y_m^{(t)} \in \{0, \dots, c\}$ is randomly sampled. Notice that the label remains fixed within a given task, but is reassigned for each new task.

Random Pixel Permuting. This environment permutes the image pixels of an image data sample. For each task, we sample a random permutation $\pi^{(t)} : \{1, \dots, d\} \rightarrow \{1, \dots, d\}$, where d is the feature dimension (i.e., the number of pixels). The permutation $\pi^{(t)}$ is applied to all images for the t th task, which yields the dataset $\mathcal{D}^{(t)} = \{(\mathbf{x}_m^{(t)}, y_m)\}_{m=1}^M$ for $\mathbf{x}_{m,i}^{(t)} = \mathbf{x}_{m,\pi^{(t)}(i)}$.

To further investigate loss of plasticity in the language models, we propose two text generation environments.

Random Seq2Seq. This environment utilizes synthetic text to evaluate the model’s ability to learn arbitrary sequence mappings. The dataset for the t th task is denoted as $\mathcal{D}^{(t)} = \{(\mathbf{x}_m^{(t)}, \mathbf{y}_m^{(t)})\}_{m=1}^M$. Both the input $\mathbf{x}_m^{(t)}$ (of sequence length p) and the target $\mathbf{y}_m^{(t)}$ (of sequence length q) consist of synthetic “words,” where each word is a random character string of fixed length L sampled from a standard alphabet.

Bigram Cipher. To evaluate generalization plasticity, we must include certain learnable patterns between input and output, as opposed to the Random Seq2Seq task. To this end, we propose the Bigram Cipher environment with a

dataset $\mathcal{D}^{(t)} = \{(\mathbf{x}_m^{(t)}, \mathbf{y}_m^{(t)})\}_{m=1}^M$. For each task t , we sample a random permutation $\pi^{(t)} : \mathcal{V} \rightarrow \{0, \dots, |\mathcal{V}| - 1\}$ over the vocabulary \mathcal{V} . The output tokens $\mathbf{y}_m^{(t)}$ is determined by the modular sum of the permuted values of the current $(\mathbf{x}_{m,i}^{(t)})$ and previous $(\mathbf{x}_{m,i}^{(t-1)})$ input tokens, where i is the i th non-whitespace letter of \mathbf{x}_m . Given an input sequence of tokens $\mathbf{x}_m^{(t)} = (\mathbf{x}_i)_{i=1}^{L_p}$, the target sequence of tokens $\mathbf{y}_m^{(t)}$ is determined by the sequence of modular sum of the permuted values of the current character $\mathbf{x}_{m,i}^{(t)}$ and the previous character $\mathbf{x}_{m,i}^{(t-1)}$: $\pi^{(t)-1}(\mathbf{y}_m^{(t)}) = (\pi^{(t)}(\mathbf{x}_{m,i}^{(t)}) + \pi^{(t)}(\mathbf{x}_{m,(i-1)}^{(t)})) \pmod{|\mathcal{V}|}$.

4. A Gradually Changing Environment

While prior work has provided fundamental insights into the phenomenon of plasticity loss, it has primarily focused on settings with abrupt task transitions. However, natural environments and human cognition often evolve in a more gradual, continuous manner over time (Mayr, 1970; Sterelny, 2011). Consequently, the discrete task boundaries used in existing benchmarks may not fully capture the dynamics of these incremental changes, leaving it an open question whether plasticity is similarly compromised in a gradually changing world.

In our work, we develop several methods to simulate a gradually changing environment. Consider the t th task represented by the dataset $\mathcal{D}^{(t)}$ and its subsequent task with dataset $\mathcal{D}^{(t+1)}$. The simulation of a gradually changing environment can be accomplished by different ways depending on the task nature.

Output Interpolation. For the Random Image Labeling environments (Dohare et al., 2021; Lewandowski et al., 2024; Lyle et al., 2022), the inputs are the same for $\mathcal{D}^{(t)}$ and $\mathcal{D}^{(t+1)}$, but the outputs become new random labels. We perform label smoothing (Müller et al., 2019) for task interpolation. Let $\alpha_t \in [0, 1]$ be an interpolation coefficient that starts from 0 and increases uniformly by a constant step size s . We have $\mathbf{y}_m^{(\alpha_t)} = (1 - 2\alpha_t)\mathbf{y}_m^{(t)} + 2\alpha_t\mathbf{u}$ for $\alpha_t \in [0, \frac{1}{2}]$, where $\mathbf{y}_m^{(t)}$ is a one-hot vector for target $\mathbf{y}_m^{(t)}$ and \mathbf{u} is a uniform distribution over the discrete target categories; for $\alpha_t \in [\frac{1}{2}, 1]$, we have $\mathbf{y}_m^{(\alpha_t)} = (2\alpha_t - 1)\mathbf{y}_m^{(t+1)} + (2 - 2\alpha_t)\mathbf{u}$ and $\alpha_{t+1} = \alpha_t + s$. In other words, we first anneal $\mathcal{D}^{(t)}$ to a uniform distribution and then anneal it to $\mathcal{D}^{(t+1)}$, offering a smooth transition from the t th task to the $(t+1)$ th task.

Input Interpolation. For the Random Image Permuting environment, the input pixel locations are shuffled in a new task, while the output remains the same. In this setting, we propose to gradually interpolate the input by direct averaging, i.e., $\mathbf{x}_m^{(\alpha)} = (1 - \alpha)\mathbf{x}_m^{(t)} + \alpha\mathbf{x}_m^{(t+1)}$. Again, α is an interpolation coefficient controlled by a step size.

It is important to note that input and output interpolations depend on the nature of the environment. In particular, they require the m th samples in $\mathcal{D}^{(t)}$ and $\mathcal{D}^{(t+1)}$ to have certain correspondence. This requirement can be reflected in certain real-world scenarios, such as changes in word meanings, where the input word is fixed while its associated meaning changes. However, such a correspondence may be unrealistic for other contexts, such as robots transitioning to a new environment, where the relationship between input and output is less predictable. To address this, we propose a general task interpolation method by annealed sampling.

Task Sampling. For more general task transitions, we sample a subset $\mathcal{D}^{(t)'}$ of size $\lceil(1 - \alpha)M\rceil$ from $\mathcal{D}^{(t)}$ and a subset $\mathcal{D}^{(t+1)'} of size $\lfloor\alpha M\rfloor$ from $\mathcal{D}^{(t+1)}$ to construct a new intermediate dataset $\mathcal{D}^\alpha = \mathcal{D}^{(t)'} \cup \mathcal{D}^{(t+1)'}$. Similar to input/output interpolation, $\alpha \in [0, 1]$ is a coefficient that starts by 0 and increments by a certain step size.$

Discussion. the observation can be used as a mitigation plan for plasticity loss in abruptly changing environments.

Theoretical Analysis. We now give an explanation of why a gradually changing environment can mitigate the loss of plasticity. Intuitively, an abrupt task change causes abrupt change of the loss landscape, and thus the parameters may be trapped in a poor local minimum in the new landscape. On the other hand, if the task changes gradually, the loss landscape also evolves gradually. With proper gradient descent, the parameters may remain in the catchment basin corresponding to the original local minimum (which is optimized for the first task). Thus, the loss of plasticity is much alleviated in such a scenario.

We provide a formal analysis under certain assumptions, such as smoothness and local convexity.

Definition 4.1 (Smoothness). Let $f : \mathbb{R}^d \rightarrow \mathbb{R}$ be a differentiable function. We say f is β -smooth ($\beta > 0$), if

$$\|\nabla f(\mathbf{x}) - \nabla f(\mathbf{y})\| \leq \beta \|\mathbf{x} - \mathbf{y}\| \quad (1)$$

for any $\mathbf{x}, \mathbf{y} \in \mathbb{R}^d$.

Definition 4.2 (Locally Strongly Convex). For a (local) minimizer \mathbf{x}_f^* of a differentiable function f , we say f is (r, μ) -strongly convex on a convex set $\mathbb{D}_{\mathbf{x}_f^*} \supseteq \{\mathbf{x} \in \mathbb{R}^d : \|\mathbf{x} - \mathbf{x}_f^*\| < r\}$, if

$$f(\mathbf{x}) \geq f(\mathbf{x}_f^*) + \langle \nabla f(\mathbf{x}_f^*), \mathbf{x} - \mathbf{x}_f^* \rangle + \frac{\mu}{2} \|\mathbf{x} - \mathbf{x}_f^*\|^2 \quad (2)$$

for any $\mathbf{x} \in \mathbb{D}_{\mathbf{x}_f^*}$. Here, $r, \mu > 0$.

We first show that, with certain constraints on step size, the parameters may converge to a local optimum without leaving a locally strongly convex region.

Lemma 4.3. Consider gradient descent (GD) starting from any point in an (r, μ) -locally strongly convex domain $\mathbb{D}_{\mathbf{x}_f^*}$ of a β -smooth function f , for some $\beta \geq \mu > 0$. Let $(\mathbf{x}_k)_{k=1}^N$ be a sequence generated by GD. If the step size satisfies $\eta \leq \min\left(\frac{1}{\beta}, \frac{r - \|\mathbf{x}_k - \mathbf{x}_f^*\|}{\beta \|\mathbf{x}_k - \mathbf{x}_f^*\|}\right)$, we have (1) \mathbf{x}_k remains within the locally strongly convex region $\mathbb{D}_{\mathbf{x}_f^*}$ in every step k of GD, and that (2) \mathbf{x}_k converges to \mathbf{x}_f^* as $k \rightarrow +\infty$.

Proof. See Appendix A.1. \square

The proof follows that for GD convergence in general, except that we need to check the radius of the locally strongly convex region.

Then, we assume that a small change of the environment has a linear form with bounded singular values. In this case, the new landscape retains smoothness and locally strongly convex properties of the previous one.

Lemma 4.4. Consider a gradually changing environment, and after one task change the loss function evolves from f to a new function g in the following form

$$g(\mathbf{x}) = f(\mathbf{W}\mathbf{x}), \quad (3)$$

where $\mathbf{W} \in \mathbb{R}^{d \times d}$ is a full-rank matrix. We assume that, under the gradually changing environment, the singular values of \mathbf{W} satisfy

$$\frac{1}{1 + \epsilon} \leq \sigma_i(\mathbf{W}) \leq \frac{1}{1 - \epsilon}, \quad \forall i \quad (4)$$

for some $\epsilon > 0$. Then, if f is β -smooth and (r, μ) -strongly convex in a local basin $\mathbb{D}_{\mathbf{x}_f^*}$, the transformed loss function g is also smooth and locally strongly convex in the corresponding local domain

$$\mathbb{D}_{\mathbf{x}_g^*} = \{\mathbf{x} : \mathbf{W}\mathbf{x} \in \mathbb{D}_{\mathbf{x}_f^*}\}, \quad (5)$$

with smoothness constant $\beta' = \beta(1 + \epsilon)^2$, strong convexity constant $\mu' = \mu \left(\frac{1}{1 + \epsilon}\right)^2$, and local convexity radius $r' = r(1 - \epsilon)$.

Proof. See Appendix A.2. \square

We can then establish that GD-updated parameters would remain in the locally strongly convex region of the new landscape g .

Lemma 4.5. Under the assumptions in Lemma 4.4, the new locally convex set $\mathbb{D}_{\mathbf{x}_g^*}$ contains \mathbf{x} if $\mathbb{D}_{\mathbf{x}_f^*}$ contains $\mathbf{W}\mathbf{x}$.

Proof. See Appendix A.3. \square

We then demonstrate that GD-optimized parameters would converge to a new local optimum of g corresponding to the previous one, i.e., $\mathbf{x}_g^* = \mathbf{W}\mathbf{x}_f^*$.

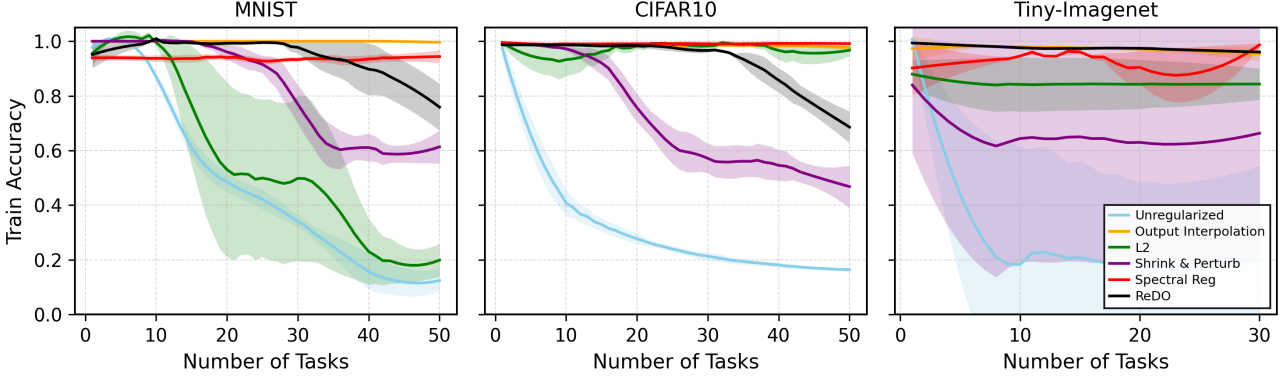


Figure 1. Trainability for Random Image Labeling tasks on MNIST and CIFAR10 using an MLP or a Resnet-18 model. Output interpolation is more effective than other plasticity mitigation methods for these vision benchmarks.

Lemma 4.6. For any $0 < c < r$ and learning rate $\eta \leq \min(\frac{1}{\beta}, \frac{r - \|\mathbf{x}_k - \mathbf{x}_f^*\|}{\beta \|\mathbf{x}_k - \mathbf{x}_f^*\|})$, the GD algorithm converges to the new minimizer $\mathbf{x}_g^* = \mathbf{W}\mathbf{x}_f^*$, as long as (1) $\frac{1}{1+\epsilon} \leq \sigma_i(\mathbf{W}) \leq \frac{1}{1-\epsilon}$ with $\epsilon = \frac{r-c}{r-c+\|\mathbf{x}_f^*\|}$ for all $i \in [d]$; and (2) the current point \mathbf{x} is close to the previous minimizer \mathbf{x}_f^* satisfying $\|\mathbf{x} - \mathbf{x}_f^*\| \leq c(1 - \epsilon)$.

Proof. See Appendix A.4. \square

Finally, we formally state our theorem below, which extends Lemma 4.6 by considering a sequence of small changes.

Theorem 4.7. Let f_0 be β_0 -smooth and (r_0, μ_0) -strongly convex. Let \mathbf{x}_0^* be a local minimizer of f_0 . We assume, under the gradually changing environment, the sequence of loss functions has the form of $f_t(\mathbf{x}_t) = f_{t-1}(\mathbf{W}_t \mathbf{x}_{t-1})$ for $t \geq 1$, where \mathbf{W}_t satisfies $\|\sigma_i(\mathbf{W}_t) - 1\| \leq \frac{r-c+\|\mathbf{x}_{t-1}^*\|}{\|\mathbf{x}_{t-1}^*\|}$, $\forall i$, for some $c \in (0, r)$. Consider $(\mathbf{x}_{t,k})_{k \in [N]}$ being a sequence generated by the GD algorithm while minimizing f_t w.r.t. \mathbf{x}_t , a learning rate $\eta \leq \min(\frac{1}{\beta_t}, \frac{r_t - \|\mathbf{x}_{t,k} - \mathbf{x}_{t-1}^*\|}{\beta_t \|\mathbf{x}_{t,k} - \mathbf{x}_{t-1}^*\|})$ of the t th task guarantees that $\mathbf{x}_{t,k}$ converges to $\mathbf{x}_t^* = \mathbf{W}_t \mathbf{x}_{t-1}^*$.

Proof. See Appendix A.5. \square

In summary, our analysis provides an explanation on why a gradually changing environment retains plasticity, as the parameters learned for the previous task can be optimized to the corresponding optimum for the new task.

5. Experiments

In this section, we empirically examine whether a gradually changing environment preserves plasticity in continual learning. We compare the following two scenarios: (1) A

gradually changing environment, and (2) An abruptly changing environment with and without loss-of-plasticity mitigation methods. In particular, we consider widely adopted and recent methods as below:

- **L2 regularization** (Krogh & Hertz, 1991), penalizing the squared magnitude of weights;
- **Shrink&Perturb** (Ash & Adams, 2020), which shrinks the model weights by a constant factor and adds noise;
- **Spectral regularization** (Lewandowski et al., 2025a), which penalizes the singular values of weight matrices; and
- Recycling dormant neurons (**ReDO**; Sokar et al., 2023), which periodically re-initializes inactive neurons.

As mentioned in Section 3, the loss of plasticity may happen in the sense of both trainability (Dohare et al., 2021; Abbas et al., 2023) and generalizability (Ash & Adams, 2020; Lee et al., 2024); they are evaluated in Subsections 5.1 and 5.2, respectively. Subsection 5.3 provides additional in-depth analyses.

5.1. Evaluation of Trainability

Trainability refers to whether the model parameters can be optimized towards new tasks, and it is a fundamental requirement for continual learning (Lyle et al., 2023; Lewandowski et al., 2025a). Extensive research in loss of plasticity has examined the ability of neural networks to retain trainability in non-stationary environments (Lyle et al., 2022; Elsayed & Mahmood, 2024; Dohare et al., 2024; Ma et al., 2024).

Tasks and Models. We experiment with the Random Image Classification and Random Seq2seq environments (task formulations presented in Section 3).

- **Random Image Labeling:** To simulate continual learning,

the Random Image Labeling environment randomly relabels the images as a new task. It has been studied the most in loss of plasticity research (Lyle et al., 2023; 2024; Lewandowski et al., 2024; Kumar et al., 2023; Tang et al., 2025) and is also adopted in our evaluation.

In particular, we consider three image benchmark datasets with increasing scales: MNIST (LeCun et al., 1998), CIFAR-10 (He et al., 2016), and Tiny-ImageNet (Le & Yang, 2015). Most previous plasticity studies have used selected datasets for their evaluation of trainability, but we include all three in our work.

For MNIST, we utilize a 4-layer Multi-Layer Perceptron (MLP) with 256 units per layer. Each hidden layer consists of a linear transformation followed by Layer Normalization and a ReLU nonlinearity. For the more complex CIFAR-10 and Tiny-ImageNet tasks, we employ an off-the-shelf ResNet-18 (He et al., 2016) architecture comprising four cascaded residual blocks with batch normalization and skip connections, totaling approximately 11 million parameters.

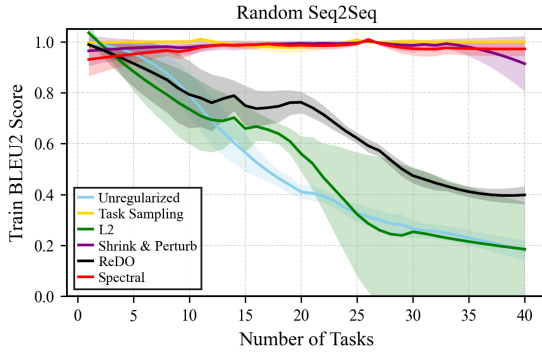


Figure 2. Trainability for random Seq2Seq task on synthetic text using T5-small. Task sampling effectively mitigates loss of trainability.

- *Random Seq2Seq*: To enrich the evaluation of trainability preservation, we propose a Random Seq2Seq environment, following the spirit of Random Image Labeling. The Random Seq2Seq environment presents a similar challenge of memorizing arbitrary mappings but in the text domain.

We adopt a pre-trained T5-small model (Raffel et al., 2020) but only keep the first Transformer block. Note that Transformers are powerful models; however, our Random Seq2Seq is synthetic and relatively simple. Therefore, we restrict the Transformer capacity to study the phenomenon of loss of plasticity in our research environment.

Results. Figure 1 and Figure 2 present the trainability results for aforementioned benchmarks.

We observe loss of trainability in all the tasks. For example, in an unregularized MLP on the Random MNIST benchmark, the training accuracy collapses from 100% to random

guessing after just 50 tasks. This is consistent with findings in the previous work that neural networks lose plasticity with abruptly changing data distribution (Dohare et al., 2021; 2024; Lyle et al., 2022; Elsayed & Mahmood, 2024; Ma et al., 2024).

We compare standard mitigation strategies designed for abrupt changes against our proposed simulation of a gradually changing environment.

Among the mitigation strategies, performance varies significantly by the architecture and benchmarks. Shrink&Perturb (Ash & Adams, 2020) and Spectral Regularization (Lewandowski et al., 2025a) excel only in the Seq2Seq language task, showing high volatility in vision benchmarks, particularly on complex datasets like Tiny-Imagenet. This disparity aligns with the findings by Bai et al., who suggest that Transformer models are inherently more robust to perturbations than CNNs (Bai et al., 2021). L2 regularized Resnet-18 sustains near perfect training accuracy for both larger vision benchmarks. However, the performance of L2 regularized MLP drops as quickly as an unregularized network, possibly due to dormant neurons and lack of skip connections. ReDO provides moderate remedy for plasticity loss in vision benchmarks via neuronal recycling; however, its performance on language tasks is less satisfactory. Previous work suggests that ReDO is ill-suited for Transformers, as the smooth nature of GELU/SiLU activations and the centering effects of Layer Normalization prevent the “dying unit” phenomenon that is common in ReLU-based CNNs (Anonymous, 2025). This phenomenon occurs when a neuron consistently outputs zero for all inputs, causing its gradient to vanish and preventing any further weight updates.

Our work investigates how a gradually changing environment affect plasticity. We find that a gradually changing environment—either simulated by output interpolation or task sampling—largely preserves the plasticity of neural networks. Output interpolation effectively preserves trainability in vision benchmarks, while task sampling is effective for language domains, matching or exceeding the performance of competing strategies. Admittedly, our simulation of gradually changing environments is not perfect, as we observe minor plasticity loss after task 35 for Random MNIST. That said, our approach still outperforms the best baseline from prior work. These results suggest that simulating a gradually changing environment is a simple yet theoretically grounded mitigation for the loss of trainability.

In summary, mitigation methods relying on resetting, regularization, or noise injection offer only partial mitigation; their strict global constraints on the optimization landscape lead to high instability. Further, these methods necessitate exhaustive hyperparameter tuning for each distinct environment; without precise calibration, their constraints often im-

pede optimization. In contrast, our simulation of a gradually changing environment provides a robust, model-agnostic solution that preserves plasticity without requiring extensive hyperparameter search.

5.2. Evaluation of Generalizability

Loss of generalizability refers to a model’s declined ability to apply learned knowledge to unseen data. While trainability is a prerequisite for generalization, prior work has largely focused on the former (Dohare et al., 2021; Lyle et al., 2022; Sokar et al., 2023; Lewandowski et al., 2024; 2025a). However, because high training accuracy can be achieved through memorization, it is critical to evaluate generalizability to confirm that the model has learned underlying patterns rather than merely overfitting the training set.

Tasks and Models. We investigate with the Random Pixel Permuting and Random Bigram Cipher environments. These permutation-based formulations, as detailed in Section 3, are particularly well-suited for evaluating generalizability because they can be applied directly to the test splits of the benchmarks.³

- **Random Pixel Permuting:** This environment random permutes the input image pixels for each task (Goodfellow et al., 2015). It is a standard benchmark for studying generalization in supervised continual learning (Dohare et al., 2024; Kumar et al., 2023; Lewandowski et al., 2025a), a protocol we similarly adopt for our evaluation. We evaluate this setting using the EMNIST dataset (Cohen et al., 2017), employing the same 4-layer MLP model utilized for the Random MNIST Labeling task.

- **Bigram Cipher:** To diversify the evaluation of generalization, we propose a Random Bigram Cipher task. This is a synthetic sequence-to-sequence task where the output sequence is generated by applying a cipher to each bigram of the input sequence. We evaluate this task using the same T5-small architecture employed in the Random Seq2Seq task.

Results. Figure 3 and Figure 4 demonstrate the generalizability results for the benchmarks described above.

In the Random Pixel Permuting task, we observe only a

³Previous work (Lewandowski et al., 2025a) has also evaluated loss of generalizability using the Vision Transformer (ViT; Dosovitskiy et al., 2021). However, we do not observe loss of generalizability in the Random Image Permuting environment if the ViT model is well-trained. Previous work only trained the model until a test accuracy of 15%, shown by Figure 1 in Page 7 and 25% shown by Figure 2 in Page 8 (Lewandowski et al., 2025a). This, unfortunately, fails to reflect the normal training of neural networks. Therefore, we exclude this setup but propose the Bigram Cipher environment, where the generalizability is genuinely lost over tasks.

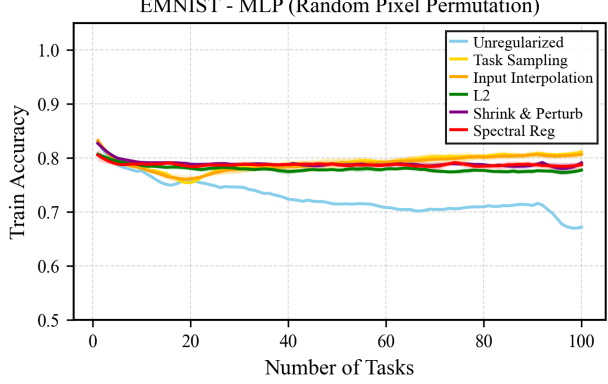


Figure 3. Continual learning with Random Pixel Permuting tasks on EMNIST using a 4-layer MLP model. Generalizability is well preserved in a gradually changing environment.

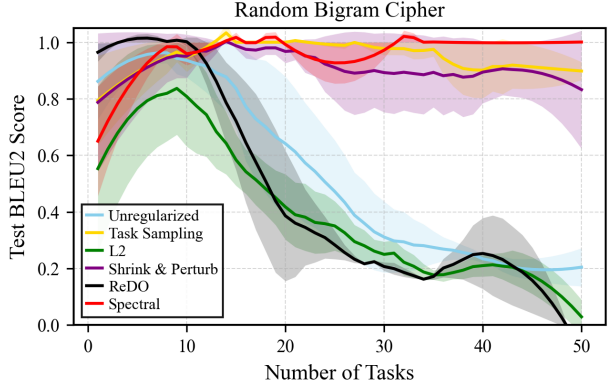


Figure 4. Generalizability evaluated by test BLEU2 score on Bigram Cipher tasks on customized T5-small model. The gradually changing environment is effective in maintaining test BLEU2 score on new tasks.

mild plasticity loss (test accuracy drops around 10%) for the unregularized MLP on the Random EMNIST benchmark with 100 tasks. Such a mild plasticity loss is consistent with previous work (Kumar et al., 2023; Lewandowski et al., 2025a), and is likely because the nature of the task allows the model to reuse previously learned image features, thereby facilitating adaptation. In this task, we observe all previously introduced mitigation methods are able to preserve plasticity to a large extent (Figure 3). Nevertheless, our task sampling and input interpolation (yellow and orange curves) remain the two most competitive methods at the 100th task.

In the Random Bigram Cipher task (Figure 4), we observe a drastic loss of generalizability for an unregularized T5-small model, with the test BLEU2 score falling to 20% after 50 tasks, reflecting high complexity of the task. Consistent with our Random Seq2Seq findings, ReDO and L2 regularization fail to retain generalizability in the language domain. Similarly, Spectral Regularization and Shrink&Perturb suc-

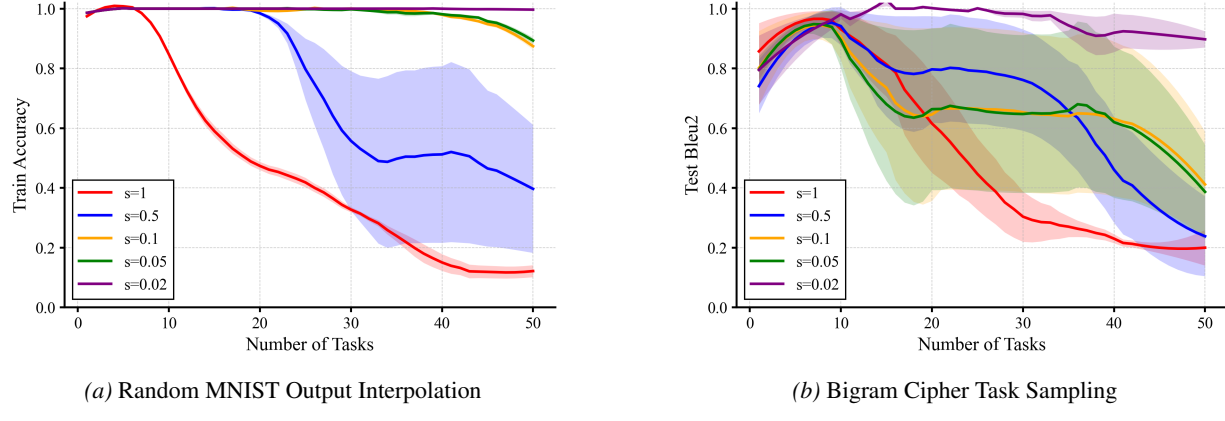


Figure 5. The effect of granularity of the interpolation step size on plasticity preservation for both trainability and generalizability task. A smaller step size simulates gradually changing environment better and retains more plasticity.

cessfully preserve generalizability, mirroring their strong performance on the Random Seq2Seq task.

Overall, our proposed simulation of a gradually changing environment preserves generalizability in both the vision task and the complex language task, matching the performance of the best-performing mitigation methods designed for abrupt task changes.

Experiment details are shown in Appendix B.

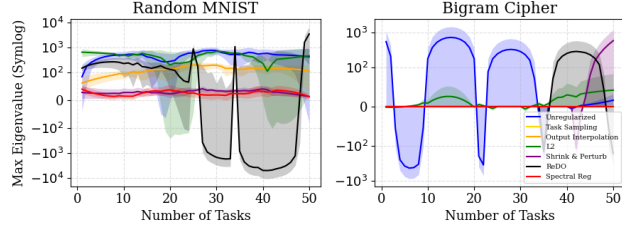


Figure 6. Maximum Eigenvalue for Random MNIST and Bigram Cipher. Interpolation and task sampling are able to keep the eigenvalues low.

5.3. In-Depth Analyses

Granularity of Interpolation and Sampling. To investigate the relationship between task transition smoothness and plasticity, we adopt two distinct experimental setups: the classic MNIST model with a 4-layer MLP model due to limited resources, and the Bigram Cipher setup with a T5-small model for generalizability. We adjust the interpolation coefficient α (as mentioned in Section 3) from 0 to 1 with a step size ranging from $\{0.02, 0.05, 0.1, 0.5\}$. As seen in Figure 5a and Figure 5b, abrupt task change (step size = 1) causes significant accuracy drop after 20 tasks for Random MNIST and 12 tasks for Bigram Cipher, respectively, while coarse-grained task change (step size = 0.5) mitigate these declines but are still not satisfactory. In comparison, step size 0.02 sustains near-perfect accuracy throughout the ex-

periments. Overall, this analysis verifies that a gradually changing environment does preserve plasticity, and that a finer-grained task transition preserves more plasticity.

Loss Landscape Geometry. To empirically characterize why gradually changing environments retain plasticity, we analyze from the loss landscape perspective. Previous work has shown that the maximum eigenvalue of the weight matrices can be interpreted as the sharpness of the loss landscape (Dinh et al., 2017; Lyle et al., 2023; Lewandowski et al., 2024). We evaluate the loss landscape geometry on a trainability task (Random MNIST) and a generalizability task (Bigram Cipher) with this metric. As shown in Figure 6, top-performing methods including Spectral Regularization and Shrink&Perturb have relatively small eigenvalues. Notably, gradual task transitions (through interpolation and task sampling) naturally maintain low and stable eigenvalues without explicit regularization penalties, suggesting a smooth landscape for optimization.

6. Conclusion

Prior plasticity research has largely focused on an artificial setup of abrupt task change, which may not fully reflect real-world continual learning scenarios. In this paper, we emphasize that real-world environments often evolve gradually. We show both theoretically and empirically that plasticity can be preserved in a gradually changing environment. Even for abruptly changing setups, loss of plasticity can be effectively mitigated by simulating gradual change from task to task through input/output interpolation and task sampling.

Impact Statement

Our work investigates neural networks' plasticity in a gradually changing environment. Although we simulate a gradually changing environment by interpolation or task sampling,

our work sheds light on real-world continual learning. The impact of our work goes beyond previous plasticity research, which mainly focuses on the contrived setting of abrupt task change.

The goal of our work is to advance the field of Machine Learning. There are many potential societal consequences of our work, none of which we feel must be specifically highlighted here.

References

Abbas, Z., Zhao, R., Modayil, J., White, A., and Machado, M. C. Loss of plasticity in continual deep reinforcement learning. In *Proceedings of The 2nd Conference on Lifelong Learning Agents*, pp. 620–636, 2023. URL <https://proceedings.mlr.press/v232/abbas23a.html>.

Anonymous. Revive and recouple: Mitigating plasticity loss in transformer architectures. In *Proceedings of The 14th International Conference on Learning Representations*, 2025. URL <https://openreview.net/forum?id=ahcb5auRmy>. Under review.

Anonymous. Activation function design sustains plasticity in continual learning. In *Proceedings of The 14th International Conference on Learning Representations*, 2026. URL <https://openreview.net/forum?id=XZf6wObHX4>. Under review.

Asadi, K., Fakoor, R., and Sabach, S. Resetting the optimizer in deep RL: An empirical study. In *Proceedings of the 37th Conference on Neural Information Processing Systems*, 2023. URL <https://openreview.net/forum?id=AnFUgNC3Yc>.

Ash, J. and Adams, R. P. On warm-starting neural network training. In *Proceedings of Advances in Neural Information Processing Systems*, pp. 3884–3894, 2020. URL https://proceedings.neurips.cc/paper_files/paper/2020/file/288cd2567953f06e460a33951f55daaf-Paper.pdf.

Bai, Y., Mei, J., Yuille, A. L., and Xie, C. Are transformers more robust than CNNs? In *Proceedings of Advances in Neural Information Processing Systems*, pp. 26831–26843, 2021. URL https://proceedings.neurips.cc/paper_files/paper/2021/file/e19347e1c3ca0c0b97de5fb3b690855a-Paper.pdf.

Bauschke, H. H., Bolte, J., and Teboulle, M. A descent lemma beyond lipschitz gradient continuity: First-order methods revisited and applications. *Mathematics of Operations Research*, 42(2):330–348, 2017. URL <https://doi.org/10.1287/moor.2016.0817>.

Berariu, T., Czarnecki, W., De, S., Bornschein, J., Smith, S. L., Pascanu, R., and Clopath, C. A study on the plasticity of neural networks. *arXiv preprint arXiv:2106.00042*, 2021. URL [url={https://arxiv.org/abs/2106.00042}](https://arxiv.org/abs/2106.00042).

Chung, W., Cherif, L., Meger, D., and Precup, D. Parseval regularization for continual reinforcement learning. In *Proceedings of Advances in Neural Information Processing Systems*, pp. 127937–127967, 2024. URL https://proceedings.neurips.cc/paper_files/paper/2024/file/e6df4efa20adf8ef9ac80e94072a429-Paper-Conference.pdf.

Citri, A. and Malenka, R. C. Synaptic plasticity: Multiple forms, functions, and mechanisms. *Neuropharmacology*, 33(1):18–41, 2008. URL <https://doi.org/10.1038/sj.npp.1301559>.

Cohen, G., Afshar, S., Tapson, J., and Van Schaik, A. EMNIST: Extending MNIST to handwritten letters. In *Proceedings of the 2017 International Joint Conference on Neural Networks*, pp. 2921–2926, 2017. URL <https://doi.org/10.1109/IJCNN.2017.7966217>.

Dean, J., Corrado, G., Monga, R., Chen, K., Devin, M., Mao, M., Ranzato, M., Senior, A., Tucker, P., Yang, K., and Ng, A. Large scale distributed deep networks. In *Proceedings of Advances in neural information processing systems*, volume 25, 2012. URL https://proceedings.neurips.cc/paper_files/paper/2012/file/6aca97005c68f1206823815f66102863-Paper.pdf.

Dinh, L., Pascanu, R., Bengio, S., and Bengio, Y. Sharp minima can generalize for deep nets. In *Proceedings of the 34th International Conference on Machine Learning*, pp. 1019–1028, 2017. URL <https://proceedings.mlr.press/v70/dinh17b.html>.

Dohare, S., Sutton, R. S., and Mahmood, A. R. Continual backprop: Stochastic gradient descent with persistent randomness. *arXiv preprint arXiv:2108.06325*, 2021. URL <https://arxiv.org/abs/2108.06325>.

Dohare, S., Hernandez-Garcia, J. F., Lan, Q., Rahman, P., Mahmood, A. R., and Sutton, R. S. Loss of plasticity in deep continual learning. *Nature*, 632(8026):768–774, 2024. URL <https://doi.org/10.1038/s41586-024-07711-7>.

Dosovitskiy, A., Beyer, L., Kolesnikov, A., Weissenborn, D., Zhai, X., Unterthiner, T., Dehghani, M., Minderer, M., Heigold, G., Gelly, S., Uszkoreit, J., and Houlsby, N. An image is worth 16x16 words: Transformers for image recognition at scale. In *Proceedings of International Conference on Learning Representations*, 2021. URL <https://openreview.net/forum?id=1gWzDwD9Dw>.

<https://openreview.net/forum?id=YicbFdNTTy>.

Elsayed, M. and Mahmood, A. R. Addressing loss of plasticity and catastrophic forgetting in continual learning. In *Proceedings of The Twelfth International Conference on Learning Representations*, 2024. URL <https://openreview.net/forum?id=sKPzAXoy1B>.

Frati, L., Craft, N., Clune, J., and Cheney, N. Reset it and forget it: Relearning last-layer weights improves continual and transfer learning. In *Proceedings of the 27th European Conference on Artificial Intelligence*, pp. 2998–3005, 2024. URL <http://dx.doi.org/10.3233/FAIA240840>.

Goodfellow, I. J., Mirza, M., Xiao, D., Courville, A., and Bengio, Y. An empirical investigation of catastrophic forgetting in gradient-based neural networks. *arXiv preprint arXiv:1312.6211*, 2015. URL <https://arxiv.org/abs/1312.6211>.

He, K., Zhang, X., Ren, S., and Sun, J. Deep residual learning for image recognition. In *Proceedings of the IEEE Conference on Computer Vision and Pattern Recognition*, pp. 770–778, 2016. URL https://openaccess.thecvf.com/content_cvpr_2016/papers/He_Deep_Residual_Learning_CVPR_2016_paper.pdf.

Kilgarriff, A. I don’t believe in word senses. *Computers and the Humanities*, 31:91–113, 1997. URL <https://doi.org/10.1023/A:1000583911091>.

Kingma, D. P. and Ba, J. Adam: A method for stochastic optimization. In *Proceedings of International Conference on Learning Representations*, 2015. URL <https://doi.org/10.48550/arXiv.1412.6980>.

Kirkpatrick, J., Pascanu, R., Rabinowitz, N., Veness, J., Desjardins, G., Rusu, A. A., Milan, K., Quan, J., Ramalho, T., Grabska-Barwinska, A., Hassabis, D., Clopath, C., Kumaran, D., and Hadsell, R. Overcoming catastrophic forgetting in neural networks. *Proceedings of the National Academy of Sciences*, 114(13):3521–3526, 2017. URL <https://www.pnas.org/doi/abs/10.1073/pnas.1611835114>.

Krogh, A. and Hertz, J. A simple weight decay can improve generalization. In *Advances in Neural Information Processing Systems*, 1991. URL https://proceedings.neurips.cc/paper_files/paper/1991/file/8eefcfdf5990e441f0fb6f3fad709e21-Paper.pdf.

Kumar, S., Marklund, H., and Roy, B. V. Maintaining plasticity in continual learning via regenerative regularization. In *Proceedings of The 3rd Conference on Lifelong Learning Agents*, 2023. URL <https://lifelong-ml.cc/Conferences/2024/acceptedpapersandvideos/conf-2024-26>.

Laurino, J., De Deyne, S., Cabana, A., and Kaczer, L. The pandemic in words: Tracking fast semantic changes via a large-scale word association task. *Open Mind*, 7:221–239, 2023. ISSN 2470-2986. URL https://doi.org/10.1162/opmi_a_00081.

Le, Y. and Yang, X. Tiny imagenet visual recognition challenge, 2015. URL https://cs231n.stanford.edu/reports/2015/pdfs/yle_project.pdf. CS231N course project, Stanford University.

LeCun, Y., Cortes, C., and Burges, C. J. C. The MNIST database of handwritten digits. <http://yann.lecun.com/exdb/mnist/>, 1998.

Lee, H., Cho, H., Kim, H., Gwak, D., Kim, J., Choo, J., Yun, S.-Y., and Yun, C. PLASTIC: Improving input and label plasticity for sample efficient reinforcement learning. In *Proceedings of The 37th Conference on Advances in Neural Information Processing Systems*, pp. 62270–62295, 2023. URL <https://openreview.net/forum?id=c5WOU7p4ES>.

Lee, H., Cho, H., Kim, H., Kim, D., Min, D., Choo, J., and Lyle, C. Slow and steady wins the race: Maintaining plasticity with hare and tortoise networks. In *Proceedings of the 41st International Conference on Machine Learning*, pp. 26416–26438, 2024. URL <https://proceedings.mlr.press/v235/lee24d.html>.

Lewandowski, A., Tanaka, H., Schuurmans, D., and Machado, M. C. Directions of curvature as an explanation for loss of plasticity. *arXiv preprint arXiv:2312.00246*, 2024. URL <https://arxiv.org/abs/2312.00246>.

Lewandowski, A., Bortkiewicz, M., Kumar, S., György, A., Schuurmans, D., Ostaszewski, M., and Machado, M. C. Learning continually by spectral regularization. In *Proceedings of The Thirteenth International Conference on Learning Representations*, 2025a. URL <https://openreview.net/forum?id=Hcb2cgPbMg>.

Lewandowski, A., Schuurmans, D., and Machado, M. C. Plastic learning with deep fourier features. In *Proceedings of The Thirteenth International Conference on Learning Representations*, 2025b. URL <https://openreview.net/forum?id=NIkfix2eDQ>.

Li, M., Zhang, T., Chen, Y., and Smola, A. J. Efficient mini-batch training for stochastic optimization. In *Proceedings of The 20th ACM SIGKDD International Conference on*

Knowledge Discovery and Data Mining, pp. 661–670, 2014. URL <https://doi.org/10.1145/2623330.2623612>.

Lyle, C., Rowland, M., and Dabney, W. Understanding and preventing capacity loss in reinforcement learning. In *Proceedings of International Conference on Learning Representations*, 2022. URL <https://openreview.net/forum?id=ZkC8wKoLbQ7>.

Lyle, C., Zheng, Z., Nikishin, E., Avila Pires, B., Pascanu, R., and Dabney, W. Understanding plasticity in neural networks. In *Proceedings of The 40th International Conference on Machine Learning*, pp. 23190–23211, 2023. URL <https://proceedings.mlr.press/v202/lyle23b.html>.

Lyle, C., Zheng, Z., Khetarpal, K., van Hasselt, H., Pascanu, R., Martens, J., and Dabney, W. Disentangling the causes of plasticity loss in neural networks. In *Proceedings of The 3rd Conference on Lifelong Learning Agents*, 2024. URL <https://lifelong-ml.cc/Conferences/2024/acceptedpapersandvideos/conf-2024-9>.

Ma, G., Li, L., Zhang, S., Liu, Z., Wang, Z., Chen, Y., Shen, L., Wang, X., and Tao, D. Revisiting plasticity in visual reinforcement learning: Data, modules and training stages. In *Proceedings of The Twelfth International Conference on Learning Representations*, 2024. URL <https://openreview.net/forum?id=0aR1s9Yx0L>.

Mayr, E. *Populations, Species, and Evolution: An Abridgment of Animal Species and Evolution*. Harvard University Press, 1970. URL <https://archive.org/details/populationsspeci0000unse/page/2/mode/2up>.

Mitra, S., Mitra, R., Maity, S. K., Riedl, M., Biemann, C., Goyal, P., and Mukherjee, A. An automatic approach to identify word sense changes in text media across timescales. *Natural Language Engineering*, 21(5):773–798, 2015. URL <https://doi.org/10.1017/S135132491500011X>.

Müller, R., Kornblith, S., and Hinton, G. E. When does label smoothing help? In *Proceedings of Advances in Neural Information Processing Systems*, 2019. URL https://proceedings.neurips.cc/paper_files/paper/2019/file/f1748d6b0fd9d439f71450117eba2725-Paper.pdf.

Nikishin, E., Schwarzer, M., D’Oro, P., Bacon, P.-L., and Courville, A. The primacy bias in deep reinforcement learning. In *Proceedings of the 39th International Conference on Machine Learning*, pp. 16828–16847, 2022. URL <https://proceedings.mlr.press/v162/nikishin22a.html>.

Obando Ceron, J., Bellemare, M., and Castro, P. S. Small batch deep reinforcement learning. In *Proceedings of Advances in Neural Information Processing Systems*, pp. 26003–26024, 2023. URL https://proceedings.neurips.cc/paper_files/paper/2023/file/528388f1ad3a481249a97cbb698d2fe6-Paper-Conference.pdf.

Raffel, C., Shazeer, N., Roberts, A., Lee, K., Narang, S., Matena, M., Zhou, Y., Li, W., and Liu, P. J. Exploring the limits of transfer learning with a unified text-to-text transformer. *Journal of Machine Learning Research*, 21(140):1–67, 2020. URL <http://jmlr.org/papers/v21/20-074.html>.

Ring, M. B. Child: A first step towards continual learning. *Machine Learning*, 28(1):77–104, 1997. URL <https://doi.org/10.1023/A:1007331723572>.

Rodriguez, J., Olabarria, M., Chvatal, A., and Verkhratsky, A. Astroglia in dementia and alzheimer’s disease. *Cell Death & Differentiation*, 16(3):378–385, 2009. URL <https://doi.org/10.1038/cdd.2008.172>.

Ruvolo, P. and Eaton, E. ELLA: An efficient lifelong learning algorithm. In *Proceedings of the 30th International Conference on Machine Learning*, pp. 507–515, 2013. URL <https://proceedings.mlr.press/v28/ruvolo13.html>.

Shin, B., Oh, J., Cho, H., and Yun, C. DASH: Warm-starting neural network training in stationary settings without loss of plasticity. In *Proceedings of The 38th Annual Conference on Neural Information Processing Systems*, 2024. URL <https://openreview.net/forum?id=IdQuUYMAlt>.

Shin, H., Lee, J. K., Kim, J., and Kim, J. Continual learning with deep generative replay. In *Proceedings of Advances in Neural Information Processing Systems*, 2017. URL https://proceedings.neurips.cc/paper_files/paper/2017/file/0efbe98067c6c73dba1250d2beaa81f9-Paper.pdf.

Sokar, G., Agarwal, R., Castro, P. S., and Evci, U. The dormant neuron phenomenon in deep reinforcement learning. In *Proceedings of the 40th International Conference on Machine Learning*, pp. 32145–32168, 2023. URL <https://proceedings.mlr.press/v202/sokar23a.html>.

Sterelny, K. From hominins to humans: How sapiens became behaviourally modern. *Philosophical Transactions of the Royal Society B: Biological Sciences*, 366(1566):809–822, 2011. URL <https://doi.org/10.1098/rstb.2010.0301>.

Tang, H., Obando-Ceron, J., Castro, P. S., Courville, A., and Berseth, G. Mitigating plasticity loss in continual reinforcement learning by reducing churn. In *Proceedings of 42nd International Conference on Machine Learning*, 2025. URL <https://openreview.net/forum?id=EkoFXfSauv>.

Thrun, S. *Lifelong Learning Algorithms*. Springer US, 1998.
URL https://doi.org/10.1007/978-1-4615-5529-2_8.

Zilly, J., Achille, A., Censi, A., and Frazzoli, E. On plasticity, invariance, and mutually frozen weights in sequential task learning. In *Proceedings of Advances in Neural Information Processing Systems*, pp. 12386–12399, 2021.
URL https://proceedings.neurips.cc/paper_files/paper/2021/file/6738fc33dd0b3906cd3626397cd247a7-Paper.pdf.

A. Proofs of Lemmas and Theorem

For completeness, we restate the descent lemma (Bauschke et al., 2017) below.

Lemma A.1 (Descent Lemma). *Let $f : \mathbb{R}^d \rightarrow \mathbb{R}$ be a differentiable function. If f is β -smooth, then for all $\mathbf{x}, \mathbf{y} \in \mathbb{R}^d$,*

$$f(\mathbf{y}) \leq f(\mathbf{x}) + \langle \nabla f(\mathbf{x}), \mathbf{y} - \mathbf{x} \rangle + \frac{\beta}{2} \|\mathbf{y} - \mathbf{x}\|^2. \quad (6)$$

Proof. Let $\mathbf{h} = \mathbf{y} - \mathbf{x}$ and define the scalar function $\phi(t) = f(\mathbf{x} + t\mathbf{h})$ for $t \in [0, 1]$. By the fundamental theorem of calculus,

$$f(\mathbf{y}) - f(\mathbf{x}) = \int_0^1 \nabla f(\mathbf{x} + t\mathbf{h})^\top \mathbf{h} dt. \quad (7)$$

Subtracting and adding $\nabla f(\mathbf{x})^\top \mathbf{h}$ inside the integral gives

$$f(\mathbf{y}) - f(\mathbf{x}) - \nabla f(\mathbf{x})^\top \mathbf{h} = \int_0^1 [\nabla f(\mathbf{x} + t\mathbf{h}) - \nabla f(\mathbf{x})]^\top \mathbf{h} dt. \quad (8)$$

Since f is β -smooth, we have $\|\nabla f(\mathbf{x} + t\mathbf{h}) - \nabla f(\mathbf{x})\| \leq \beta t \|\mathbf{h}\|$. Applying the Cauchy–Schwarz inequality and integrating over $t \in [0, 1]$ yields

$$f(\mathbf{y}) - f(\mathbf{x}) - \nabla f(\mathbf{x})^\top \mathbf{h} \leq \int_0^1 \beta t \|\mathbf{h}\|^2 dt = \frac{\beta}{2} \|\mathbf{h}\|^2. \quad (9)$$

Rearranging the terms gives the desired result. \square

A.1. Proof of Lemma 4.3

Proof. From the GD update $\mathbf{x}_{k+1} = \mathbf{x}_k - \eta \nabla f(\mathbf{x}_k)$ and β -smoothness of f ,

$$\|\nabla f(\mathbf{x}_k)\| \leq \beta \|\mathbf{x}_k - \mathbf{x}_f^*\|. \quad (10)$$

Thus,

$$\|\mathbf{x}_{k+1} - \mathbf{x}_f^*\| \leq \|\mathbf{x}_k - \mathbf{x}_f^*\| + \eta \|\nabla f(\mathbf{x}_k)\| \leq (1 + \eta \beta) \|\mathbf{x}_k - \mathbf{x}_f^*\|. \quad (11)$$

The step-size constraint guarantees that $\|\mathbf{x}_{k+1} - \mathbf{x}_f^*\| \leq r$, ensuring that $\mathbf{x}_k \in \mathbb{D}_{\mathbf{x}_f^*}$ for all k (condition 1).

For convergence, using μ -strong convexity of f within $\mathbb{D}_{\mathbf{x}_f^*}$, we have

$$\|\mathbf{x}_{k+1} - \mathbf{x}_f^*\|^2 \leq (1 - \mu\eta) \|\mathbf{x}_k - \mathbf{x}_f^*\|^2, \quad (12)$$

which implies geometric decay and $\mathbf{x}_k \rightarrow \mathbf{x}_f^*$ as $k \rightarrow \infty$ (condition 2). \square

A.2. Proof of Lemma 4.4

Proof. The gradient of g is $\nabla g(\mathbf{x}) = \mathbf{W}^\top \nabla f(\mathbf{W}\mathbf{x})$. For any $\mathbf{x}, \mathbf{y} \in \mathbb{R}^d$,

$$\|\nabla g(\mathbf{x}) - \nabla g(\mathbf{y})\| = \|\mathbf{W}^\top (\nabla f(\mathbf{W}\mathbf{x}) - \nabla f(\mathbf{W}\mathbf{y}))\| \leq \|\mathbf{W}\|^2 \cdot \beta \|\mathbf{x} - \mathbf{y}\| \leq \beta(1 + \epsilon)^2 \|\mathbf{x} - \mathbf{y}\|, \quad (13)$$

so g is $\beta' = \beta(1 + \epsilon)^2$ -smooth.

Next, since f is μ -strongly convex,

$$f(\mathbf{W}\mathbf{x}) \geq f(\mathbf{W}\mathbf{y}) + \nabla f(\mathbf{W}\mathbf{y})^\top (\mathbf{W}\mathbf{x} - \mathbf{W}\mathbf{y}) + \frac{\mu}{2} \|\mathbf{W}(\mathbf{x} - \mathbf{y})\|^2. \quad (14)$$

By the chain rule, $\nabla g(\mathbf{y}) = \mathbf{W}^\top \nabla f(\mathbf{W}\mathbf{y})$, and using $\|\mathbf{W}(\mathbf{x} - \mathbf{y})\| \geq \sigma_{\min}(\mathbf{W}) \|\mathbf{x} - \mathbf{y}\| \geq \frac{1}{1 + \epsilon} \|\mathbf{x} - \mathbf{y}\|$, we have

$$g(\mathbf{x}) \geq g(\mathbf{y}) + \nabla g(\mathbf{y})^\top (\mathbf{x} - \mathbf{y}) + \frac{\mu}{2} \left(\frac{1}{1 + \epsilon} \right)^2 \|\mathbf{x} - \mathbf{y}\|^2. \quad (15)$$

Thus g is (r', μ') -locally strongly convex with $\mu' = \mu(1 + \epsilon)^{-2}$.

Finally, for any \mathbf{x} satisfying $\|\mathbf{x} - \mathbf{x}_g^*\| \leq r' = r/\sigma_{\max}(\mathbf{W})$, we have $\|\mathbf{W}\mathbf{x} - \mathbf{x}_f^*\| \leq \|\mathbf{W}\| \cdot \|\mathbf{x} - \mathbf{x}_g^*\| \leq \sigma_{\max}(\mathbf{W}) r' = r$, which implies $\mathbf{W}\mathbf{x} \in \mathbb{D}_{\mathbf{x}_f^*}$. Hence $\mathbf{x} \in \mathbb{D}_{\mathbf{x}_f^*}$, completing the proof. \square

A.3. Proof of Lemma 4.5

Proof. For any $\mathbf{x} \in \mathbb{R}^d$ satisfying $\|\mathbf{x} - \mathbf{x}_g^*\| \leq r(1 - \epsilon)$, we have

$$\|\mathbf{W}\mathbf{x} - \mathbf{x}_f^*\| = \|\mathbf{W}(\mathbf{x} - \mathbf{x}_g^*)\| \leq \|\mathbf{W}\| \|\mathbf{x} - \mathbf{x}_g^*\| \leq \frac{1}{1-\epsilon} r(1 - \epsilon) = r. \quad (16)$$

Hence $\mathbf{W}\mathbf{x} \in \mathbb{D}_{\mathbf{x}_f^*}$, which implies $\mathbf{x} \in \mathbb{D}_{\mathbf{x}_g^*}$. Therefore, the ball of radius $r(1 - \epsilon)$ around \mathbf{x}_g^* is fully contained within the preimage of the strongly convex basin $\mathbb{D}_{\mathbf{x}_f^*}$. \square

A.4. Proof of Lemma 4.6

Proof. Under the spectral bounds on \mathbf{W} , the shift between the two minimizers is bounded by

$$\|\mathbf{x}_f^* - \mathbf{x}_g^*\| = \|\mathbf{x}_f^* - \mathbf{W}^{-1}\mathbf{x}_f^*\| \leq \|\mathbf{I} - \mathbf{W}^{-1}\| \|\mathbf{x}_f^*\| \leq \epsilon \|\mathbf{x}_f^*\| \leq (r - c)(1 - \epsilon). \quad (17)$$

If $\|\mathbf{x} - \mathbf{x}_f^*\| \leq c(1 - \epsilon)$, then by the triangle inequality,

$$\|\mathbf{x} - \mathbf{x}_g^*\| \leq \|\mathbf{x} - \mathbf{x}_f^*\| + \|\mathbf{x}_f^* - \mathbf{x}_g^*\| \leq (r - c)(1 - \epsilon) + c(1 - \epsilon) = r(1 - \epsilon), \quad (18)$$

which implies $\mathbf{x} \in \mathbb{D}_{\mathbf{x}_g^*}$ by Lemma 4.5. Since g is smooth and locally strongly convex in $\mathbb{D}_{\mathbf{x}_g^*}$, the standard GD convergence result (Lemma 4.3) ensures that $\mathbf{x}_k \rightarrow \mathbf{x}_g^*$ for a valid step size $\eta \leq 1/\beta$. Note that the effective smoothness β may vary slightly as the environment evolves. \square

A.5. Proof of Theorem 4.7

Proof. We begin with \mathbf{x}_0^* , a benign minimizer of f_0 , and initialize GD within its locally strongly convex and β -smooth basin $\mathbb{D}_{\mathbf{x}_0^*}$. When the loss transitions from f_0 to $f_1(\mathbf{x}) = f_0(\mathbf{W}_1\mathbf{x})$, the spectral constraint on \mathbf{W}_1 ensures the minimizer shift is bounded:

$$\|\mathbf{x}_0^* - \mathbf{x}_1^*\| = \|\mathbf{x}_0^* - \mathbf{W}_1^{-1}\mathbf{x}_0^*\| \leq \|\mathbf{I} - \mathbf{W}_1^{-1}\| \|\mathbf{x}_0^*\| \leq \epsilon \|\mathbf{x}_0^*\| \leq (r - c)(1 - \epsilon). \quad (19)$$

During optimization, Lemma 4.3 guarantees that the GD iterates \mathbf{x}_k contract toward \mathbf{x}_0^* , eventually satisfying $\|\mathbf{x}_k - \mathbf{x}_0^*\| \leq c(1 - \epsilon)$. By Lemma 4.6, this implies $\mathbf{x}_k \in \mathbb{D}_{\mathbf{x}_1^*}$, ensuring convergence to the new minimizer \mathbf{x}_1^* .

Assuming the result holds for \mathbf{x}_i^* , the same argument applies recursively to the transition $f_i \mapsto f_{i+1}$ under the corresponding \mathbf{W}_{i+1} satisfying the same spectral condition. By induction, GD converges to each successive shifted minimizer $\mathbf{x}_1^*, \mathbf{x}_2^*, \dots, \mathbf{x}_t^*$. \square

B. Experiment Details

All experiments were optimized using Adam (Kingma & Ba, 2015). The learning rate was selected via an initial sweep over $\{0.005, 0.001, 0.0005, 0.0001\}$. We found that a learning rate of 0.001 performed best for MNIST, Tiny-ImageNet, and the Bigram Cipher task, while 0.0001 was optimal for the remaining experiments. All results are averaged over 5 random seeds, and shaded regions in figures indicate the standard error of the mean.

Datasets and hyperparameters:

MNIST. MNIST consists of 28×28 grayscale images from 10 classes. We uniformly sampled 5120 training examples across classes and used a batch size of 512. All mitigation methods were trained for 240 epochs per task.

CIFAR-10. CIFAR-10 contains 32×32 color images from 10 classes. All 50,000 training images were used. We employed a batch size of 250 and trained for 120 epochs per task.

Tiny-ImageNet. Tiny-ImageNet consists of 64×64 color images spanning 200 classes. All 100,000 training samples were used. We used a batch size of 250 and trained for 120 epochs per task for the Random Image Labeling setting.

Language Tasks:

- **Random Seq2Seq.** Synthetic text data were generated from the English alphabet with word length 5, sentence length 50, target length 5, and 5120 total samples. Models were trained with a batch size of 64 for 900 epochs per task.
- **Bigram Cipher.** Synthetic text data were generated from the English alphabet with word length 5, sentence length 10, target length 10. 1280 total samples were generated for training and 512 for testing. We used a batch size of 64 and trained for 200 epochs per task.